

The role of spatial correlations in same-material tribocharging

Galien Grosjean,* Sebastian Wald, Juan Carlos Sobarzo, and Scott Waitukaitis

IST Austria
Lab Building West
Am Campus 1
3400 Klosterneuburg AT
(Dated: September 3, 2022)

The observation of charge mosaics suggests that same-material tribocharging may arise via surface heterogeneity, whose origin and role have gone unquestioned. Here we reveal how spatial correlations in donor/acceptor properties affect the surface heterogeneity model. Correlations dramatically enhance the scale of charge transfer, while effectively inhibiting fluctuations. A toy model based on a generic nucleation process where donors prefer to be close is sufficient to explain our results and previous experiments, giving insight in the underlying cause and effect of surface heterogeneity.

Tribocharging, the transfer of charge between materials during contact, plays a critical role in natural phenomena [1–5], industrial processes [6, 7], and energy harvesting devices [8–10], yet its causes are not well-understood [11]. For insulators, issues as fundamental as which species is being transferred (electrons *vs.* ions) are ongoing topics of debate [11–13]. Furthermore, there is overwhelming evidence that even identical materials, when brought into contact, systematically transfer charge [14–23]. Several mechanisms could be involved in this ‘same-material’ tribocharging, including ones based on localized stresses [24], trapped electrons [25–29], induced polarization [30–34], or mechanochemistry [6, 35–37]. Alternatively, a few experiments suggest that the required symmetry breaking could be more subtle, involving inherent statistical fluctuations in the properties of the material itself [17, 18, 22, 38, 39]. Working with conformally contacting PDMS samples, Apodaca *et al.* found that the scale of charge transfer grows with the square root of the contacting area [17]. This led them to propose the existence of heterogeneity in the charge donor/acceptor nature of the surface. Imagining a surface of area $A = L \times L$ can be partitioned into equally sized donor/acceptor sites and assuming they are *uncorrelated* and Gaussian distributed, one naturally recovers $|\Delta Q| = C\sqrt{A}$, where the prefactor, C , depends on the site density, N/A . Physically, this density must have a lower limit on the order of one donor/acceptor per atom, yet the density ($2.90 \times 10^{18} \text{ mm}^{-2}$) required to explain the data in Ref. [17] corresponds to sites whose side lengths are approximately 0.005 \AA —more than 100 times smaller than the Bohr radius of hydrogen.

Nonetheless, qualitative features reminiscent of this surface-heterogeneity-based model have been observed, but at significantly larger lengthscales. Using Kelvin Force Probe Microscopy, Baytekin *et al.* observed neighboring regions of positive and negative charge on samples after contact that were correlated over lengths from tens to hundreds of nanometers [18]. The existence of these ‘charge mosaics’ raises numerous questions. How can the unrealistically small lengthscales implied by Ref. [17]

be rationalized with the much larger scales observed in Ref. [18]? How would the existence of spatial correlations alter the surface heterogeneity model? And what

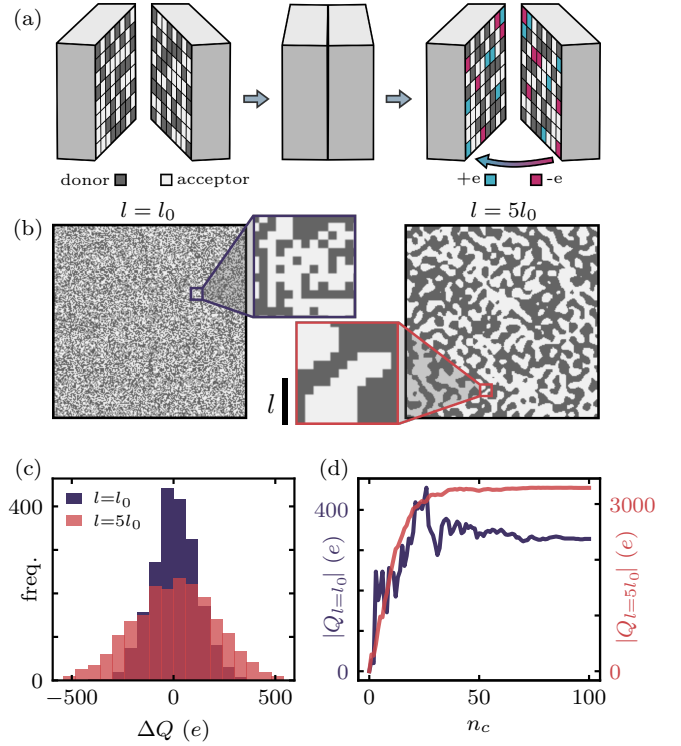


FIG. 1. (a) Same-material tribocharging may be caused by inherent surface heterogeneity [17]. Partitioning the surface into equally sized sites, a unit charge e is transferred when any donor site touches an acceptor; the net transfer, ΔQ , is in general non-zero due to statistical variations. (b) Surfaces with identical donor probability p (and acceptor probability $1 - p$), but different correlation lengths, l ; on the left, $l = l_0$ (where l_0 is the size of a single donor/acceptor site), and on the right $l = 5l_0$. (c) The distribution in ΔQ for a single contact is broader when $l = 5l_0$ (dark violet, $\sim 200 e$) than when $l = l_0$ (light red, $\sim 100 e$). (d) For sequential contacts, the scale of charge transfer is again larger for $l = 5l_0$, and fluctuations that dominate the $l = l_0$ case are not significant.

underlying physical process(es) could create such heterogeneity in the first place? In this work, we use simulations and analysis to investigate how spatial correlations in donor/acceptor properties affect the surface heterogeneity model for same-material tribocharging. We find that the scale of charge transferred is dramatically enhanced, growing approximately linearly with the correlation length when it is much larger than the elementary site size. For sequential contacts, we determine how correlations affect the average behavior, but also how they effectively suppress fluctuations. Finally, we address the origin of the the underlying heterogeneity, revealing that a nucleation toy model where donor sites ‘prefer’ to be close is sufficient to explain the observed behavior.

We simulate charge transfer between pairs of ‘synthetic’ surfaces (in contrast with the physically derived surfaces discussed later) by creating two N -element matrices involving three lengthscales: l_0 , l , and L . The smallest scale, l_0 , corresponds to an elementary donor/acceptor site and is represented by a single matrix element. The largest scale, L , corresponds to the system size. We assume that there is a single intermediate scale, l , which characterizes the donor/acceptor correlations. Each matrix element is assigned to be either a donor or an acceptor, with probabilities p and $1 - p$, respectively. Critically, these assignments take into account correlations over the lengthscale l , which is accomplished via appropriate thresholding on a random scalar field (see Supplemental Material [40]). During a ‘contact’, we generate a ‘left’ surface and a ‘right’ surface with distinct donor/acceptor patterns, but generated from identical input lengthscales and probabilities. Charge transfer of one unit, e , between matrix elements ij occurs if and only if (1) element ij on the left/right is a donor, (2) element ij on the right/left is an acceptor, (3) the value of an independent random uniform variable is less than the transfer probability, α , and (4) in the case of sequential contacts, transfer between sites ij has not previously occurred. The net charge transferred is the difference in the total numbers of left-to-right (‘right’) and right-to-left (‘left’) transfers.

Figure 1 illustrates two representative surfaces, where in the first $l = l_0$, and in the second $l = 5 l_0$. In each case, the *a priori* probability that an individual element will be a donor/acceptor is the same ($p = 0.5$). Nonetheless, we see stark differences in the charge transfer between pairs with $l = l_0$ compared to pairs with $l = 5 l_0$. In Fig. 1c, we plot distributions of the amount of charge transferred in the first contact, ΔQ , for ensembles consisting of 1000 pair-instances. Both of the resulting distributions are Gaussian and centered at zero, but while the $l = l_0$ distribution has a width of $\sim 100 e$, the $l = 5 l_0$ width is $\sim 200 e$. The lengthscale l also affects the behavior in sequential contacts for a given surface pair. Fig. 1d shows two examples of the accumulated charge on one surface, $|Q|$, as a function of the number of contacts, n_c . Like

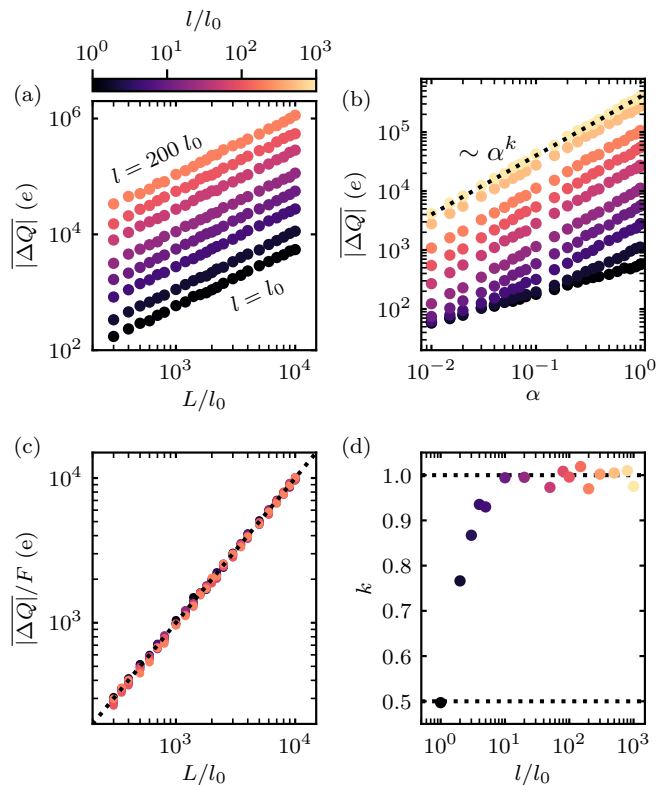


FIG. 2. (a) Average charge transfer $|\Delta Q|$ after one contact, for different values of l and L ($\alpha = 1$, $p = 0.5$). The scaling $|\Delta Q| \propto L$ is recovered in all cases, but with a growing prefactor. (b) For fixed L and l , $|\Delta Q| \propto \alpha^k$, where the exponent k is a function of l . (c) The data from (a) for $l \gg l_0$ collapses to a line of slope unity when rescaled using Eq. 2. (d) The exponent k vs. l/l_0 . When $l \approx l_0$, transfer is probabilistic (Eq. 1) and $|\Delta Q| \propto \sqrt{\alpha}$. When $l \gg l_0$, we can treat transfer as occurring at a fixed rate (Eq. 2) where $|\Delta Q| \propto \alpha$.

the initial ΔQ , the final charge, Q_f , is typically much larger when $l = 5 l_0$. Additionally, fluctuations from one contact to the next are on the order of Q_f for the $l = l_0$ case, but are hardly discernible when the $l = 5 l_0$ (consistent with the smooth curves that have been observed experimentally [17]).

In Fig. 2, we examine the scale of charge transfer from the first contact in detail. Fig. 2a shows the average absolute value of charge exchanged, $|\Delta Q|$, as a function of increasing system size and for several values of l . The scaling $|\Delta Q| \propto \sqrt{A} \propto L/l_0$ is recovered in all cases, but the prefactor steadily increases with $l > l_0$. Fig. 2b shows that the dependence on the transfer probability, α , exhibits unexpected non-linear behavior. At every value of l , we see a trend consistent with a power law, *i.e.* $|\Delta Q| \propto \alpha^k$. However, the exponent, k , increases with l , starting at $k = 0.5$ for $l = l_0$ and saturating at $k = 1.0$ for $l \gg l_0$ (Fig. 2d).

To explain these observations, we first consider the case $L \gg l = l_0$, here sketching our arguments and present-

ing a detailed explanation in the Supplemental Material [40]. Our analysis runs parallel to Ref. [17], but with the aid of our simulations we have teased out subtleties that were previously missed. We momentarily focus solely on right transfers, which occur with a compound probability $p(1-p)\alpha$. Absent spatial correlations, the behavior of site ij is independent of its neighbors, hence the total number of right transfers is Gaussian distributed with mean $eNp(1-p)\alpha$ and width $e\sqrt{Np(1-p)\alpha(1-p(1-p)\alpha)}$. A similar distribution exists for left transfers, but strictly speaking these are only valid when considered independently as simultaneous left/right transfer cannot occur. Nonetheless, this would only happen with probability $(p(1-p)\alpha)^2$, which is inherently small. We can therefore approximate the left/right distributions as independent. Given ΔQ is the difference of left/right transfers, it is also Gaussian distributed, with zero mean and a width given by $\sigma = e\sqrt{2Np(1-p)\alpha(1-p(1-p)\alpha)}$. Neglecting terms on the order of $(p(1-p)\alpha)^2$ and considering $|\overline{\Delta Q}| = \sqrt{2/\pi}\sigma$ [40], we arrive at

$$|\overline{\Delta Q}| = \sqrt{\frac{2}{\pi}} \frac{eL}{l_0} \sqrt{2p(1-p)\alpha}. \quad (1)$$

This result therefore recovers the \sqrt{A} scaling found previously [17], but differs in that the α dependence is square root rather than linear—consistent with the low l/l_0 limit $k = 0.5$ in Fig. 1d. Physically, this reflects the fact that, at the level of elementary charged particles, transfer is inherently probabilistic. In the Supplemental Material [40], we verify that Eq. 1 collapses our numerically simulated data in this limit for a wide range of values of p and α .

Next we consider the case $L \gg l \gg l_0$ (again leaving the detailed treatment to the Supplemental Material [40]). This fundamentally alters the argument above, as we cannot assume that the left/right behavior of a given site is independent of its neighbors. We therefore break the problem into two parts. First, we deal with the (correlated) donor/acceptor probabilities by considering a system rescaled by the factor l/l_0 , leading to new surfaces with $N' = N/(l/l_0)^2$ larger ‘patches’. With the only spatial structure involving the introduction of this scale (and not, *e.g.*, periodicity), we make the ansatz that donor/acceptor identities of entire patches can be presumed to occur with probabilities p and $1-p$. Next, we rescale back to the original system to deal with the (uncorrelated) transfers, which still occur independently for each site and with probability α . During contact, the characteristic number of donors that face acceptors in the patches is given by $n = (l/l_0)^2$. If n is sufficiently large, the mean transfer per patch (αn) is much larger than the fluctuations ($\sqrt{n\alpha(1-\alpha)}$), which means we can treat α as a rate rather than a probability. Considering this, we find that the scale of charge transfer when $l \gg l_0$ is

given by

$$|\overline{\Delta Q}| = \sqrt{\frac{2}{\pi}} \frac{e\alpha Ll}{l_0^2} \sqrt{2p(1-p)}. \quad (2)$$

This expression differs from Eq. 1 in two ways. First, the dependence on α is linear rather than square root (explaining the large l/l_0 limit $k = 1$ in Fig. 2d). This is the same as Ref. [17], but is only justified if correlations are present. Second, unlike both Eq. 1 and Ref. [17], the scale of transfer increases linearly with the ratio of the correlation length to the site size, l/l_0 . In Fig. 2c, we confirm that rescaling the data from Fig. 2a by the prefactor $F = \alpha l/l_0 \sqrt{4p(1-p)}/\pi$ collapses $|\overline{\Delta Q}|$ when $l \gg l_0$. The increase of charge transfer with l is somewhat surprising, especially considering that the mean number of donors/acceptors on a surface remains constant. The fundamental reason for this is that the variability in the number of donors/acceptors depends strongly on the scale of spatial correlations. This can be readily appreciated by considering the extreme case $l = L$, where all N sites are either donor or acceptor, and consequently $|\overline{\Delta Q}| \propto \alpha eN$. This highlights the fact that, in the surface heterogeneity framework, same- and different-material tribocharging are two manifestations of the same phenomenon, only appearing to be different as a result of the scale at which one looks.

We now turn our attention to sequential contacts. As shown in Fig. 3a, repeated transfer between the same two surfaces leads to curves in total accumulated charge, $|Q|$ vs. n_c , that saturate at some value, Q_f . For large or small l/l_0 , the underlying trend is consistent with a saturated exponential, *i.e.*,

$$Q(n_c) = Q_f (1 - \exp(-\alpha n_c)). \quad (3)$$

Previous studies have integrated $|Q|$ vs. n_c curves numerically [17], or simply assumed a form similar to Eq. 3 [38], but in the Supplemental Material we show this is straightforward to recover [40]. What is more interesting are the relative fluctuations on approach to Q_f . For large l/l_0 , these are not noticeable, with curves that neatly approximate Eq. 3. On the other hand, for small l/l_0 , the early charging behavior is overwhelmed by the fluctuations, with non-monotonic features that are not observed experimentally [17]. We quantify the scale of the fluctuations by repeatedly performing first contacts between a single pair of surfaces (‘resetting’ each time, as in Fig. 3b), measuring the resulting single-pair fluctuations, δQ , and then repeating over many pairs to calculate the ensemble average, $\overline{\delta Q}$. In Fig. 3c we show the behavior of δQ for a few pair instances, which reveals that the fluctuations grow with L and depend strongly on α , but are seemingly independent of l .

To understand why, we note that for a particular surface pair the donor/acceptor arrangement is fixed, which means the fluctuations must arise solely from the transfer probability, α . Denoting the number of donors on the

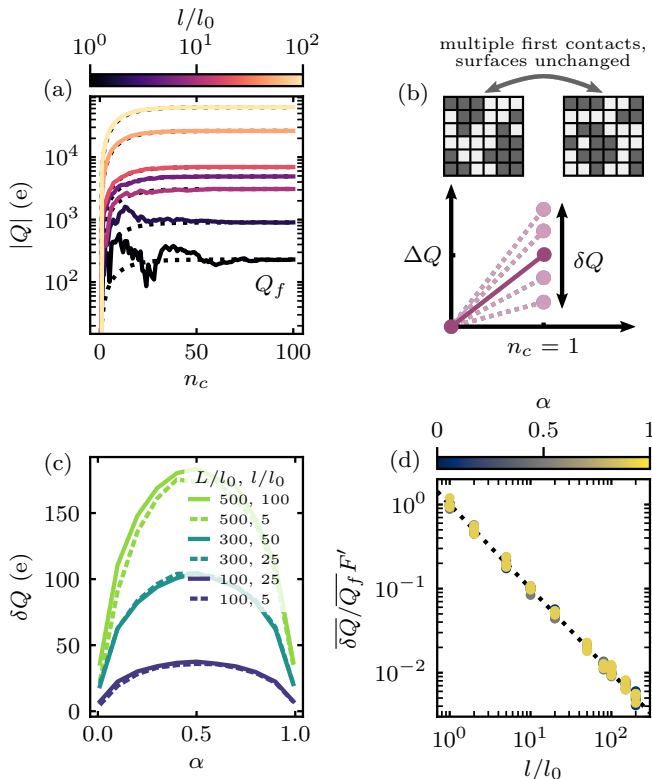


FIG. 3. (a) Sequential contacts between two surfaces leads to accumulated charge transfer, $|Q|$, which increases until it saturates at Q_f (shown here for several l/l_0 and with $\alpha = 0.1$ and $p = 0.5$). For small l/l_0 , fluctuations are on the order of Q_f , overwhelming the underlying trend and leading to non-monotonic behavior, whereas for large l they are hardly noticeable. Dotted lines correspond to Eq. 3 using the measured Q_f . (b) We quantify the fluctuations by repeating the first contact between the same two surfaces several times and measuring the spread, δQ . (c) For a particular surface pair, δQ depends on both α and L , but is largely independent of l , leading to the smoother charging observed in (a) as well as Fig. 1. (d) As $Q_f \propto l/l_0$, the relative fluctuations decrease with l , leading to the smoother charging observed in (a) as well as Fig. 1. Each point corresponds to the ensemble average over 20 pairs of surfaces of the fluctuations over 50 contacts.

left/right that face acceptors on the right/left as N_{\rightleftharpoons} , it can be shown that $\delta Q = e\sqrt{(N_{\leftarrow} + N_{\rightarrow})\alpha(1-\alpha)}$. In the Supplemental Material [40], we justify how we can simply use the average values for $\bar{N}_{\rightleftharpoons} = (L/l_0)^2 p(1-p)$ to arrive at an approximate expression for the ensemble,

$$\overline{\delta Q} = e \frac{L}{l_0} \sqrt{2p(1-p)\alpha(1-\alpha)}. \quad (4)$$

This equation establishes that the fluctuations, like the charge transfer, grow linearly with L , but are *independent* of l . The counter-intuitive conclusion is that while the relative influence of fluctuations cannot be suppressed by increasing the system size, this can be achieved by increasing spatial correlations. We find the ratio $\overline{\delta Q}/\overline{Q_f} = \sqrt{\alpha(1-\alpha)\pi/2}/(l/l_0) = F'/(l/l_0)$ which we use to rescale

and collapse data in Fig. 3d, confirming that the relative fluctuations quickly diminish with l . Assuming reasonable α , we have $\delta Q/Q_f \sim 1$ when $l \sim l_0$, validating our simulation results that fluctuations dominate the sequential contact behavior when no correlations are present.

Surface heterogeneity inherently features nontrivial spatial correlations, which we have shown have significant quantitative consequences on charge transfer. However, the most fundamental question remains unaddressed: what is the underlying cause of the surface heterogeneity in the first place? Though experiments should ultimately decide, we propose that a generic nucleation process where donors prefer to be near other donors is a viable candidate. We support this by developing time-dependent and latticed-based simulations that mimic a physical process to create surfaces, again resulting in $L/l_0 \times L/l_0$ donor/acceptor matrices. At each time step, a donor site has a probability of transitioning into an acceptor site, and vice-versa. Critically, these probabilities are determined by the states of the neighboring sites due to energetic interactions, *i.e.*,

$$\begin{aligned} P_A(\nu) &= P_0 \exp(-K\nu) \\ P_D(\nu) &= P_0 \exp(-K(4-\nu)), \end{aligned} \quad (5)$$

where ν is the number of first neighbors that are donors (*i.e.* $\nu \in [0, 4]$; see the Supplemental Material [40]). Physically, these equations represent a system where each additional neighbor modifies the relative energy barrier for nucleation/disappearance by a constant $\epsilon/kT = K$. Though more involved versions of this type of model have been developed, we choose this simple form with the aim of identifying basic ingredients sufficient to cause surface structures to emerge. Full simulation details can be found in the Supplemental Material [40].

Starting with some initial donor/acceptor arrangement, we let a surface evolve until it reaches a dynamic equilibrium that depends on the parameters in Eq. 5. Three examples corresponding to different K are shown in Fig. 4a. A movie showing the evolution of a surface is also included in the Supplemental Material [40]. To characterize these surfaces in the context of our preceding analysis, we directly measure p and l/l_0 . Determining p is trivial. To determine l/l_0 we define the radial correlation function,

$$C(r) = \langle s(R)s(R+r) \rangle - \langle s(R) \rangle \langle s(R+r) \rangle, \quad (6)$$

where s is the site identity (1 for donor and 0 for acceptor) at a position R on the surface, r is the distance away from the point R , and averages denoted by $\langle \rangle$ are over all pairs of points separated by r . Figure 4b shows an example of $C(r)$ calculated for a particular surface. We use the first zero crossing (within the margin of error) to define the correlation length, l , as it corresponds to the typical distance before having an equal probability of switching from a donor to an acceptor (or *vice versa*). In

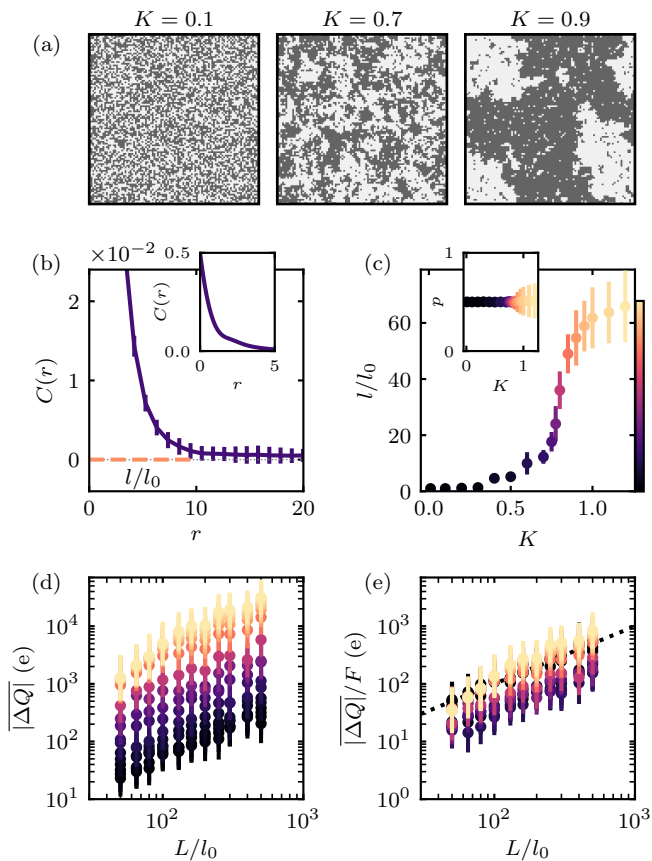


FIG. 4. (a) A generic nucleation process can lead to patches with a given size $l > l_0$. (b) We measure l/l_0 using the radial correlation function (Eq. 6). We keep the same color scale for l/l_0 in all subfigures. (c) We vary l/l_0 through parameter K in Eq. 5. The inset shows that p remains constant. (d) As before, the charge transferred after a contact is drastically increased by the introduction of a lengthscale. (e) We verify that Eq. 2 is still valid. The dotted line is the identity line.

the Supplemental Material, we show that this definition identically recovers the known correlation lengths in our synthetic surfaces for Figs. 1-3 [40]. In Figure 4c, we show how sweeping through the parameter K allows us to explore different values of l/l_0 ranging from 1 to ~ 60 , with $p \approx 0.5$ and holding P_0 fixed.

We use these simulated surfaces as input for contact experiments, with the rules for charge transfer the same as described previously. We generate 20 surfaces for various combinations of correlation length l/l_0 and surface size L/l_0 , and calculate $|\Delta Q|$ as before for every permutation of two surfaces (Fig. 4d). One sees immediately that the qualitative effect of the spatial correlations in this physically derived system is the same as what we showed for the synthetic surfaces in Fig. 2a, *i.e.* the scale of transfer increases with the correlation length. Figure 4e presents the results rescaled using Eq. 2, which largely collapses them onto a single line with the predicted unity slope. In the Supplemental Material [40], we explain how the

slight deviation for intermediate values of l/l_0 is due to the presence of a spectrum of lengthscales in our simulated surfaces. The presence of multiple lengthscales was also noted in experiments [18]. Unsurprisingly, these points correspond to the region where the slope of l/l_0 *vs.* K is sharpest and, consequently, the variability in the size of generated features can be expected to be largest.

Our work in this letter ultimately stems from three well-supported assumptions: first, that charge transfer between insulators occurs locally [17, 22, 28, 29, 38, 39]; second, that the transfer of a single charge carrier is probabilistic [41, 42]; and third, that at least in some circumstances, same-material charge transfer involves surface heterogeneity [17, 18]. Based on these assumptions, we have shown that spatial correlations play a crucial role. In a single contact, they directly affect the amount of charge transferred, leading to approximately linear growth when $l \gg l_0$. In sequential contacts, they diminish the relative importance of fluctuations, leading to the smooth Q *vs.* n_c curves that are observed experimentally. Our results allow us to quantitatively resolve the inconsistency regarding the site size mentioned in the introduction. Specifically, fitting the data from [17] with our form in Eq. 2 and using the larger lengthscale ($l \approx 450$ nm) measured by [18], we extract a single site size of $l_0 \approx 4$ Å, which corresponds to the much more plausible value of one donor/acceptor on an area the size of several atoms (see Supplemental Material [40]). This point highlights the importance of spatial resolution in charge transfer simulations—for quantitative agreement, the correlation length must be resolved. Finally, we have addressed the origins of the surface heterogeneity, showing that a nucleation mechanism that energetically favors neighboring donors is sufficient to explain the previous experimental results and our analysis/simulations. Our toy model is generic enough to be consistent with proposed mechanisms such as adsorption of some donor/acceptor (*e.g.* H₂O) from the surrounding environment [22, 38, 43], although unlike previous results ours illustrates that neighboring sites cannot be treated as independent. Our model may also be consistent with unexplored possibilities such as donor/acceptor recruitment during surface formation (*e.g.* from the bulk during the curing of polymers). Experiments capable of directly addressing the role of such mechanisms in the charging process are required for further progress.

This project has received funding from the European Unions Horizon 2020 research and innovation programme under the Marie Skłodowska-Curie Grant Agreement No. 754411.

* galienmariep.grosjean@ist.ac.at

- [1] T. Steinpilz, K. Joeris, F. Jungmann, D. Wolf, L. Brendel, J. Teiser, T. Shinbrot and G. Wurm, *Nat. Phys.* **16**, 225-229 (2020).
- [2] S.J. Desch and J.N. Cuzzi, *Icarus* **143**, 87-105 (2000).
- [3] G. Wurm, L. Schmidt, T. Steinpilz, L. Boden and J. Teiser, *Icarus* **331**, 103-109 (2019).
- [4] D.L. Schrader, K. Nagashima, S.R. Waitukaitis, J. Davidson, T.J. McCoy, H.C. Connolly Jr., and D.S. Lauretta, *Geochim. Cosmochim. Ac.* **223**, 405-421 (2018).
- [5] P. Berdeklis and R. List, *J. Am. Met. So.* **58**, 2751-2770 (2001).
- [6] H.T. Baytekin, B. Baytekin, T.M. Hermans, B. Kowalczyk and B.A. Grzybowski, *Science* **341**, 1368-1371 (2013).
- [7] T. Abbasi and S.A. Abbasi, *J. Hazard. Mat.* **140** 7-44 (2007).
- [8] M. Kanik, O. Aktas, H.S. Sen, E. Durgun and M. Bayindir, *ACS Nano* **8**, 9311-9323 (2014).
- [9] U.G. Musa, S.D. Cezan, B. Baytekin and H.T. Baytekin, *Sci. Rep.* **8**, 2472 (2018).
- [10] Z.L. Wang, *ACS Nano* **7** 9533-9557 (2013).
- [11] D.J. Lacks and T. Shinbrot, *Nat. Rev. Chem.* **3**, 465-476 (2019).
- [12] C. Liu and A.J. Bard, *J. Am. Chem. Soc.* **131**, 6397-6401 (2009).
- [13] B. Baytekin, H.T. Baytekin and B.A. Grzybowski, *J. Am. Chem. Soc.* **134**, 72237226 (2012).
- [14] P.E. Shaw, *Nature* **118**, 659-660 (1926).
- [15] J. Lowell and W.S. Truscott, *J. Phys. D: Appl. Phys.* **19**, 1273-1280 (1986).
- [16] K.M. Forward, D.J. Lacks and R.M. Sankaran, *Geophys. Res. Lett.* **36**, L13201 (2009).
- [17] M.M. Apodaca, P.J. Wesson, K.J.M. Bishop, M.A. Ratner and B.A. Grzybowski, *Angew. Chem. Int. Ed.* **49**, 946-949 (2009).
- [18] H. T. Baytekin, A. Z. Patashinski, M. Branicki, B. Baytekin, S. Soh and B. A. Grzybowski, *Science* **333**, 308-312 (2011).
- [19] W. Hu, L. Xie and X. Zheng, *Appl. Phys. Lett.* **101**, 114107 (2012).
- [20] S.R. Waitukaitis and H.M. Jaeger, *Rev. Sci. Instrum.* **84**, 025104 (2013).
- [21] S.R. Waitukaitis, V. Lee, J.M. Pierson, S.L. Forman and H.M. Jaeger, *Phys. Rev. Lett.* **112**, 218001 (2014).
- [22] L. Xie, N. Bao, Y. Jiang and J. Zhou, *AIP Adv.* **6**, 035117 (2016).
- [23] V. Lee, N.M. James, S.R. Waitukaitis and H.M. Jaeger, *Phys. Rev. Mat.* **2**, 035602 (2018).
- [24] P. E. Shaw, *Proc. Phys. Soc.* **39**, 449 (1926).
- [25] J. Lowell and W. S. Truscott, *J. Phys. D: Appl. Phys.* **19**, 1281 (1986).
- [26] D. J. Lacks, N. Duff and S. K. Kumar, *Phys. Rev. Lett.* **100**, 188305 (2008).
- [27] D. J. Lacks and A. Levandovsky, *J. Electrostat.* **65**, 107-112 (2007).
- [28] N. Duff and D.J. Lacks, *J. Electrostat.* **66**, 51-57 (2008).
- [29] D.J. Lacks and R.M. Sankaran, *Particul. Sci. Technol.* **34**, 55-62 (2016).
- [30] T. Shinbrot, M. Rutala and H. Herrmann, *Phys. Rev. E* **96**, 032912 (2017).
- [31] T. Siu, J. Cotton, G. Mattson and T. Shinbrot, *Phys. Rev. E* **89**, 052208 (2014).
- [32] J. Kolehmainen, A. Ozel, Y. Gu, T. Shinbrot and S. Sundaresan, *Phys. Rev. Lett.* **121**, 124503 (2018).
- [33] R. Yoshimatsu, N.A.M. Araújo, G. Wurm, H.J. Herrmann and T. Shinbrot, *Sci. Rep.* **7**, 39996 (2016).
- [34] R. Yoshimatsu, N.A.M. Araújo, T. Shinbrot and H.J. Herrmann, *Soft Mat.* **12**, 62616267 (2016).
- [35] M. Sow, D.J. Lacks and M.R. Sankaran, *J. Appl. Phys.* **112**, 084909 (2012).
- [36] M. Sow, R. Widenor, A. Kumar, S.W. Lee, D.J. Lacks and R.M. Sankaran, *Angew. Chem. Int. Ed.* **51**, 2695 (2012).
- [37] M. Sow, D.J. Lacks and R.M. Sankaran, *J. Electrostat.* **71**, 396399 (2013).
- [38] I.A. Harris, M.X. Lim and H.M. Jaeger, *Phys. Rev. Mat.* **3**, 085603 (2019).
- [39] H. Yu, L. Mu and L. Xie, *J. Electrostat.* **90**, 113-122 (2017).
- [40] See Supplemental Material at [URL will be inserted by publisher] for additional details.
- [41] D.J. Lacks and M.R. Sankaran, *J. Phys. D: Appl. Phys.* **44**, 453001 (2011).
- [42] J.F. Kok and D.J. Lacks, *Phys. Rev. E* **79**, 051304 (2009).
- [43] M.D. Hogue, E.R. Mucciolo, C.I. Calle and C.R. Buhler, *J. Electrostat.* **63**, 179-188 (2005).